RF PHOTONICS

Contents

Executive Summary

Photonics and Radio Frequency (RF) are two key communication technologies, usually associated to wired and wireless transmission media respectively due to the low transmission losses at their respective frequency range. Current wired links use optical fibers which exhibit transmission losses as low as 0.2 dB/km at 1500 nm wavelength (193 THz). Wireless links are dominated by RF-domain microwave frequencies (3 GHz – 30 GHz) with atmospheric attenuation below 0.1 dB/km. As RF engineers have moved up into higher frequency bands, the complementarity between the two technologies has been used to advantageously combine the best of both worlds to deliver RF systems with unmatched performance, especially regarding bandwidth, with the ultimate objective of achieving the wired-wireless convergence [1]. This combination has led to the development of the RF Photonics field, widely known as Microwave Photonics (MWP) although its scope of RF frequencies has expanded beyond the microwave range into the millimeter-wave (mmW, 30 GHz – 300 GHz) and Terahertz (THz, 300 GHz – 10 THz) regions of the spectrum. The historical difficulty to deliver systems operating within these bands has coined the term 'Terahertz gap'.

Its initial key advantage was the low propagation loss in optical fiber links to distribute microwave signals without the losses of coaxial cables. From this simple application, the field emerged enabling RF signals to be generated, distributed, processed, and analyzed using advantages of photonic technologies to provide functions that are very complex or even impossible to carry out directly in the RF domain [2]. More recently, with the RF fronthaul of mobile networks moving into the millimeter-wave (30 to 300 GHz) and Terahertz (300 GHz to 3 THz) ranges [3], the two technologies are being brought closer, enabling the RF photonics field to reach into a broader range of applications, including sensing, instrumentation, imaging, and spectroscopy, all of which are keys to addressing societal challenges. RF photonic technology recently is even being considered and demonstrated to do sensing in the optical domain. Examples are FMCW LiDAR and optical sensors that have RF outputs (e.g., photoacoustic sensors, optical-fiber sensors). Moreover, optical wireless communication (aka LiFi), as complementary communication solution to RF connectivity through WiFi at several GHz bands (2,4 GHz – 5 GHz), is being explored by companies such as PureLiFi, amongst others, for short range indoor and even for long range satellite communication applications. RF photonics is also finding applications in aerospace, as described in IPRS-I Aerospace chapter.

Current RF photonic systems are based on discrete components linked through optical fiber, which limits energy-efficiency, flexibility and scalability, and, as a result, high volume application. These limitations can be addressed through wafer-based photonic integration technology, developing these systems using photonic integrated circuits (PICs). The added benefits of using integration technology are amongst reduced costs: (a) reduced Size, Weight, and Power consumption (SWaP), (b) Improved performance, (c) Reduced number of optical and/or electrical interfaces, and (d) Realization of new functionalities.

Introduction

RF Photonics (also generally known as Microwave Photonics, MWP) is an inter-disciplinary field that bridges photonics together with RF engineering. It aims to apply photonic solutions to RF applications in order to achieve superior performance in terms of bandwidth, insertion loss, dynamic range, size, weight, efficiency, and power, and of course, eventually achieved at lower cost and scalable volumes.

MWP serves as an enabling technology in a wide variety of applications such as high-speed wireless communication networks, radar systems and sensors. The implementation of RF photonics technology is paramount for meeting the communication demands of future systems. These systems are requiring more data throughput, larger operating bandwidths, higher operating frequencies, better sensitivity, and better image processing with higher resolution. These requirements must be achieved at a lower cost and reduced size, weight, and power consumption. Radar systems and sensors benefit from the low frequency-dependent loss and low dispersion offered by MWP. The low loss of fiber optic cables makes possible distributed sensors that can be located far apart from each other and that

can even be operated in a coherent manner. The low dispersion makes possible wideband steering of RF beams and multi-band operation of sensor systems.

Thanks to the availability of telecom-based high-frequency components such as lasers, modulators and photodiodes, photonics have spearheaded the access to the higher bands of the RF frequency spectrum. Currently there are several photonic techniques for the generation of Continuous-Wave (CW) signals, with frequencies ranging from the microwave to the Terahertz regions of the spectrum. Photonics also can accomplish frequency translation: up-conversion from a lower RF frequency to a higher RF frequency and down-conversion from a higher RF frequency to a lower RF frequency. Photonic techniques are superior to conventional electronic ones with respect to the range of frequencies that can be addressed (broadband devices), especially for frequency tunable generators and up/down converters. Moreover, optical signals for producing the millimeter/terahertz-wave signals can be distributed over long distances via fiber optic cables.

Furthermore, RF photonics technology is used to perform signal processing functions in the optical domain that facilitate and complement the additional signal processing done with RF electronics. These functions include frequency-selective filtering and cancellation, spectral shaping, power limiting, sampling, frequency up/down conversion, and waveform matching.

Integrated Microwave/Millimeter-wave Photonics (IMWP) seeks to address the limitations of current MWP systems, which are based on separately packaged photonic components connected through optical fibers, by using photonic integrated circuits that comprise multiple photonic components interconnected by on-chip optical waveguides. This leads to significant reduction in cost, power consumption and fiber connection failures all of which help with industrial implementation in higher volume. IMWP is still at its infancy and a considerable body of knowledge, technical and scientific road mapping and interactions between industry and academia need to be developed during the next years [4].

Situational (Infrastructure) analysis

The major functions of RF photonics systems include photonic generation, processing, control and distribution of radio frequency signals. In general, there are two main types of MWP systems. On one hand, the MWP transmitter, photonic techniques can up-convert an electronic data signal into the RF domain, generating the modulated RF carrier frequency in the optical domain. On the other, the MWP receiver, photonic techniques can down-convert the modulated RF carrier to an Intermediate-Frequency (IF) or to a baseband (BB) electronic signal.

The general structure of a RF photonic transmitter system includes the building blocks shown in Figure 1, such as:

- Optical signal generator, usually based on infrared lasers emitting at 1500 nm, producing continuous-wave single wavelength laser light or short optical pulses at a defined repetition rate. This is a crucial difference establishing two types of MWP systems, frequency-domain or time-domain.
- An optical modulator, which performs the Electrical-to-Optical (E/O) conversion used to bring the high-speed data signals into the optical domain,
- Optical amplification, used to compensate for the insertion losses (signal propagation losses) of the optical functional building blocks, which can be placed at any point in the optical path
- Optical signal processing unit, which can perform an added functionality (RF up/down conversion, optical filtering, optical delay, optical beam forming …) in the optical domain, and
- An Optical-to-Electrical (O/E) converter, to generate the RF signals in the electrical domain, followed by an electrical RF amplifier and an antenna element to radiate the RF.

It is worth noting that the different optical building blocks shown in Figure 1 (signal generator, modulator, amplifier and signal processing and O/E converter) can either be realized through discrete components which are fiber-connected or be integrated monolithically as a photonic integrated circuit (PIC). Where the optical fiber might be located in this block diagram is not a straightforward matter. Deciding which building blocks are best integrated together and which blocks are required to be separated by optical fiber depends not only on fabrication technology,

but also on the constraints of the target application. For example, in the application scenario of a remote antenna radio head of a mobile wireless fronthaul, it only makes sense to integrate the O/E converter, RF amplifier and antenna since these three blocks need to be located at the remote antenna site away from the rest of building blocks to which are connected by an optical fiber. However, for other applications such as millimeter-wave radar, all four blocks might be part of the same photonic integrated circuit chip or module.

The other MWP system is the RF photonic receiver. Figure 2 shows two configurations of a RF photonic receiver. One configuration is based on a high-speed photo-mixer coupled to a photonic local oscillator for optoelectronic down-conversion of THz data signals to an intermediate frequency band that is easily accessible by conventional electronics. By tuning the frequency of the photonic local oscillator, the receiver can cover a wide range of carrier frequencies. The most common detector has been photoconductive antenna devices [5], although photodiodes have also been reported operating as a photonic downconverter [6][7]. Photoconductive devices are fabricated on Low Temperature GaAs (LT-GaAs), and more recently on InP and iron (Fe) doped InGaAs, not all of which are easily integrated. Novel types of O/E converters, such as the plasmonic internal-photoemission detectors (PIPEDs)[8], are currently being developed to enable RF Photonic transmitter and receiver integration on a silicon photonic platform. The other configuration of a RF photonic receiver, also shown in Figure 2, has blocks that are similar to those in a RF photonic transmitter.

The important figures of merit for the MWP systems are link gain, noise figure and phase noise, input/output intercept points, spurious free dynamic range (SFDR), and output power. These metrics show the impact of losses, noise, and nonlinearities [2]. The relative importance of these metrics and the specific values that are desired for the metrics depend on the application. For example, a Radio-over Fiber (RoF) link that carries digital or PAM-4 signals modulated on a RF carrier would have a different requirement for the SFDR than a radar link. A link for generation of a millimeter-wave signal for transmission from an antenna may have a strong requirement on the saturation power but not necessarily on the SFDR.

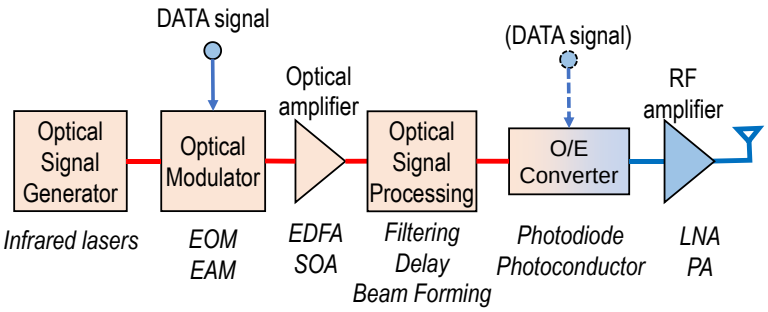

Figure 1 *Schematic of the building blocks of a RF Photonic transmitter. EOM: electro-optic modulator, EAM: electro-absorption modulator, EDFA: Erbium-doped fiber amplifier, SOA: semiconductor optical amplifier, LNA: low-noise amplifier, PA: power amplifier.*

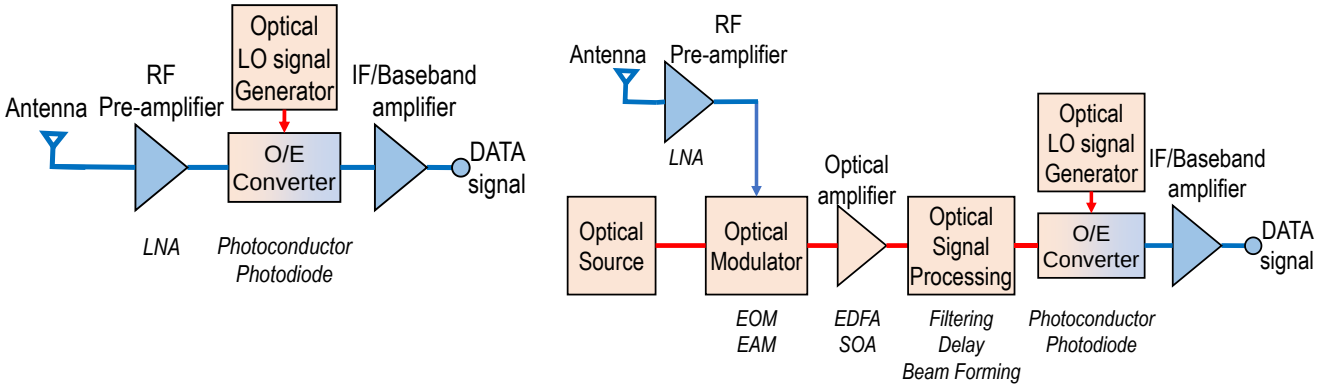

Figure 2 *Schematic of the building blocks of a RF Photonic receiver based on: (a) Photomixer detector, and (b) RF-to-Optical direct detection. LNA: low-noise amplifier, IF: intermediate frequency, EOM: electro-optic modulator, EAM: electro-absorption modulator, EDFA: Erbium-doped fiber amplifier, SOA: semiconductor optical amplifier.*

OPTICAL SIGNAL GENERATION

The optical signal generator building block is where the RF photonic approach presents two key advantages over all-electronics approaches, namely (i) the bandwidth, (ii) the maximum reachable RF frequency and (iii) the wide frequency tuning range. Currently, there are a number of different photonic-based RF signal generation techniques, which as shown in Figure 3, can be organized in two main categories: optical heterodyne and pulsed.

Optical heterodyne technique

Optical heterodyne is a Continuous-Wave (CW) RF signal generation technique based on mixing two optical wavelengths λ_1 and λ_2 on a photo-mixer (photodiode or photoconductor), generating an electrical output signal at the difference frequency of the optical wavelengths, $f_{beat} = c|\lambda_1 - \lambda_2|/(\lambda_1 \lambda_2)$. There are different solutions for generating the two optical wavelengths. The most straightforward method combines the light output from two different single-frequency semiconductor lasers as shown in Fig. 4(a). It is the simplest and also the most cost-effective technique, which does not require electrical devices operating at high frequencies. While its main advantages are the maximum achievable RF frequency and the broad frequency tuning range, the frequency stability is generally poor if the two lasers are free-running, generating a wide electrical beat-note linewidth with a large

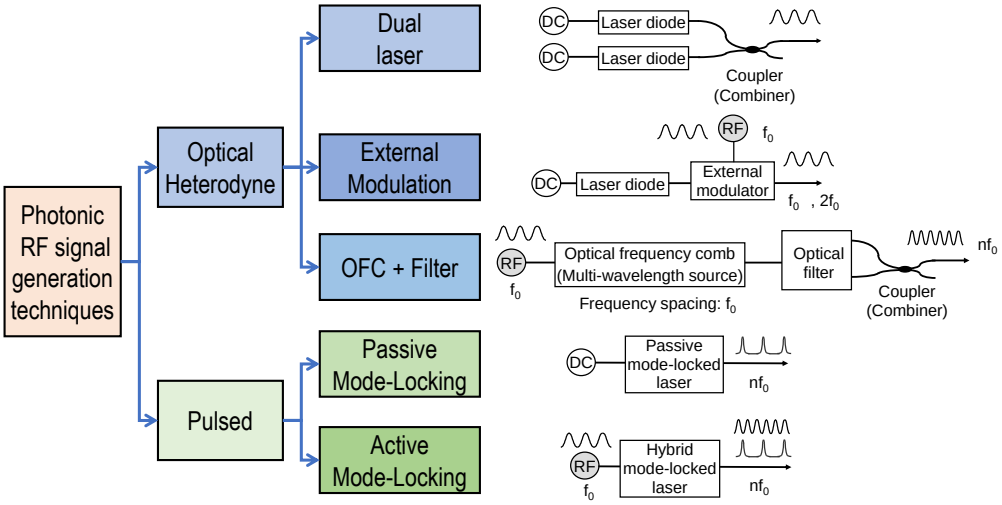

Figure 3 *Schematic diagram of different photonic-based RF signal generation techniques. OFC: optical frequency comb, f_0: fundamental frequency from electronic RF synthesizer, nf_0: n^{th}-harmonic of electronic RF synthesizer frequency.*

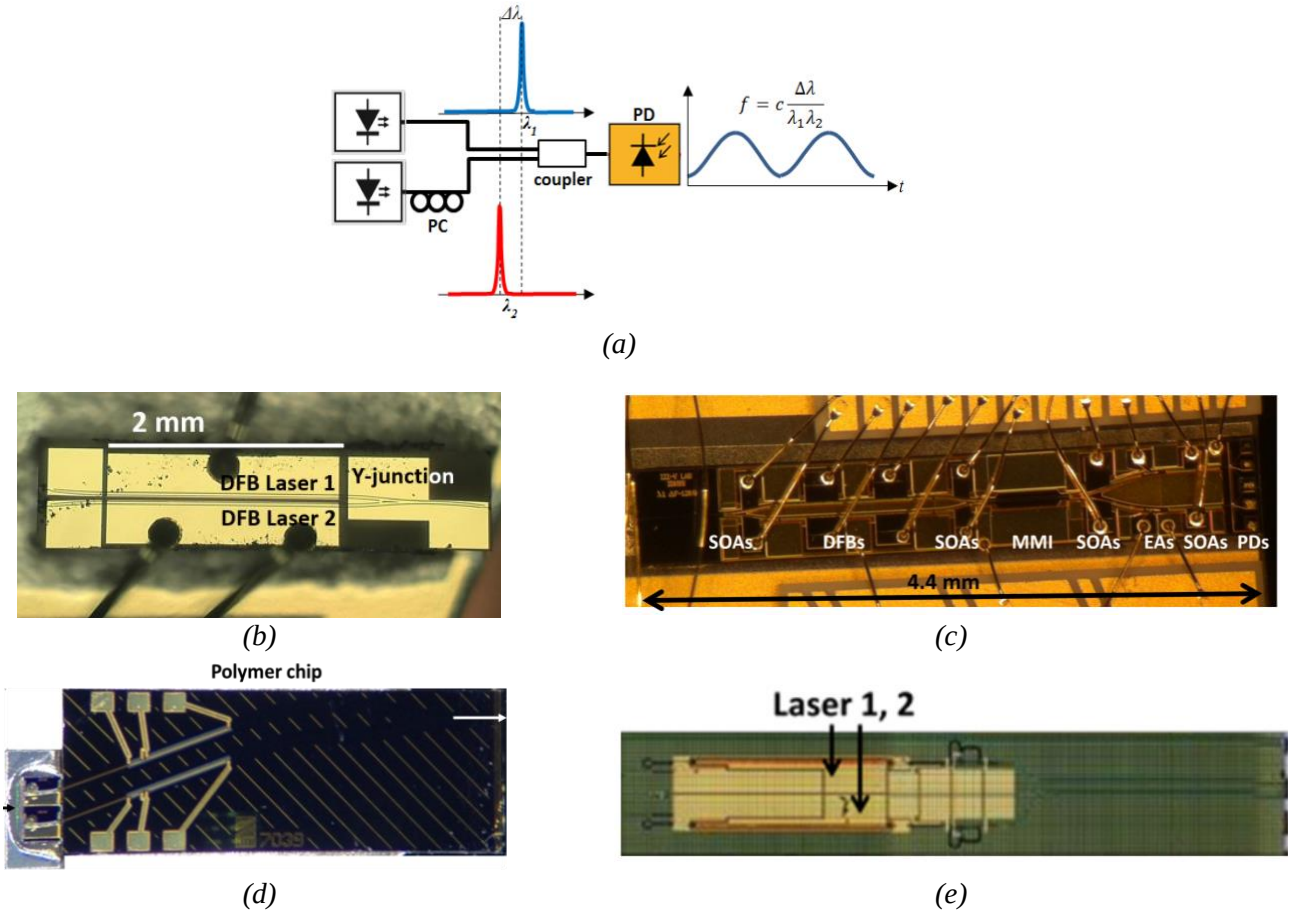

Figure 4 *Photonic optical heterodyne signal generation system: (a) key building blocks, including two single-wavelength lasers, at least one being wavelength tunable, an optical combiner (coupler) and a photodiode (PD), (b) realization by integration of two DFB lasers and optical combiner [10], (b) fully monolithic MWP transmitter with two DFB lasers, MMI combiner [12], (c) hybrid InP/Polymer integration of two DFB and optical combiner [15], and (c) silicon/III-V heterogeneous MWP transmitter [14].*

frequency drift (> 10 MHz/h). Phase locking schemes (optical injection locking, optical phase locked loop [9]) have been commonly used to lock the two optical wavelengths in phase, increasing the RF signal stability.

Photonic integration has been a key technology for improving the stability of optical heterodyne sources through two main aspects [10]: a) The two laser sources being on the same chip allows them to share the same Peltier cooler experiencing the same environmental fluctuations, and b) The distances become shorter, which helps to improve the efficiency of delay sensitive electronic Optical Phase-Locked-Loop (OPLL) [11]. Indium-Phosphide (InP) monolithic integration of two DFB lasers has been demonstrated, as shown in Fig. 4(b), thereby reducing the linewidth below 300 kHz for cavity lengths of 2500-µm and achieving RF beat note linewidths below 1-MHz for frequencies ranging from 2.5 GHz to 20 GHz [10]. With this approach, a fully integrated millimeter-wave transmitter on InP was demonstrated, shown in Fig. 4(c), which includes two DFB lasers, 2x2 Multimode Interference (MMI) couplers, Semiconductor Optical Amplifiers (SOAs), Electro-Absorption Modulators (EAM) and Uni-Travelling Carrier Photodiodes (UTC-PD) [12]. The wavelength tuning range of each DBF laser was about 1.5 nm (~ 188 GHz) and the optical linewidth was greater than 1 MHz. The advantage of the integrated approach was demonstrated when the frequency tuning range was extended above 2 THz by integrating a four DFB laser array combining standard optical element building blocks (BB) from an InP photonic integration foundry platform [13]. Currently, hybrid integration technology has also been considered for integrating optical heterodyne generators. A photonic microwave generator on a heterogeneous silicon-InP platform was demonstrated, with lasers that tune over 42 nm and having less than 150 kHz linewidth, generating RF signals from 1 to 112 GHz [14]. Terahertz signal generation at 330 GHz was demonstrated using an InP/Polymer hybrid integrated optical heterodyne source, including two Distributed Bragg Reflector (DBR) lasers and a Y-junction optical combiner [15].

These lasers, with a wavelength tuning range of 50 nm and optical linewidth of 2.8 MHz, were injection locked to an Optical Frequency Comb (OFC) to generate a 330 GHz beat note signal with 12 kHz linewidth. As shown in Fig. 5 (reproduced from [16]), hybrid and heterogeneous integration technologies are enabling a route to reducing the optical linewidth of integrated lasers, which is crucial for high quality optical heterodyne techniques. Linewidths of individual lasers down to few hundred Hertz have been demonstrated. The key point is now how to reduce the relative variations between the two lasers.

An alternative solution for improving the stability of the optical heterodyne technique is to use a different method to achieve a dual wavelength signal for optical heterodyning based on external modulation [17]. This technique makes use of a Continuous-Wave (CW) laser followed by a Mach-Zehnder Modulator (MZM), as shown schematically in Fig. 3. With this approach, the phase noise of the generated signal depends directly on the phase noise of the RF generator providing the modulation signal driving the MZM. By selecting the modulator bias point and modulator structure, double-sideband suppressed carrier (DSB-SC) modulation is achieved, generating two optical wavelengths at twice the RF synthesizer frequency, thereby doubling the frequency of the CW synthesizer. Higher multiplication factors can be achieved by taking advantage of the inherent nonlinearity of the optical modulator response to generate high-order optical sidebands. Quadrupling of the CW synthesizer has been reported. To date, all of these demonstrations have been based on commercially available discrete components.

External modulation provides the best optical heterodyne RF signal quality, with the two optical wavelengths being referenced to the same CW RF synthesizer. However, higher frequencies can only be achieved with increasingly complex structures to obtain higher multiplication factors. An alternative for achieving higher frequencies with the high signal quality of external modulation is to use an optical frequency comb generator (OFCG) followed by an optical filter. The OFCG is an optical source producing a large number of optical wavelengths which have a fixed frequency spacing between them, with the key characteristic being that the wavelengths of the spectral comb are phase locked. The optical filter, which selects two of these wavelengths with the desired spacing, can be implemented as an arrayed waveguide grating (AWGs) or other tunable optical filter that selects any two wavelengths of the OFC. The combination of two modes from the OFCG at a photodetector generates an optical heterodyned signal whose frequency is equal to the frequency spacing of the two selected optical modes of the comb. Although there is a growing number of OFCG implementations, the most common to date is using a single-mode laser and optical amplitude and/or phase modulators which generate multiple optical sidebands around the optical carrier frequency, with a frequency spacing defined by the RF frequency driving the modulator. With this approach, using either an optical or an electrical tunable filter at the system output, a reconfigurable RF signal generator can be realized, whose output carrier frequency is an integer multiple of the RF frequency driving the modulator. However, phase noise performance of such a solution depends on the multiplication factor M, with respect to the fundamental driving RF frequency, i.e., the obtained phase noise power spectral density is equal to M^2 times the phase noise of the employed driving RF signal, similar to any nonlinear electronic frequency multiplier. Currently it is becoming more common to obtain optical combs produced by non-linear optical methods such as the Kerr combs resulting from four wave mixing in micro-ring resonators. Micro-integration technology has been used to generate a comb of frequencies across 50 nm of the optical spectrum which

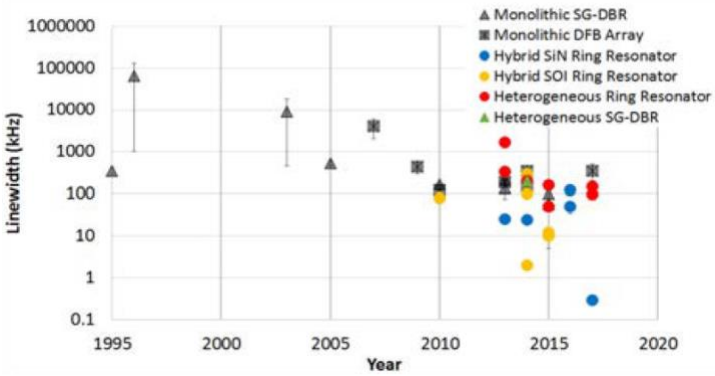

Figure 5 *Linewidth of widely tunable integrated lasers versus time. Monolithic is III–V-integration, hybrid is individual III–V dies bonded, soldered or butt-coupled to another substrate material, and heterogeneous larger pieces of the III–V gain material are bonded to silicon. SG–DBR: Sampled grating distributed bragg reflector, DFB: distributed feedback, SiN: silicon-nitride, SOI: silicon-on-insulator.(from [16])*

allows locking of a semiconductor laser to any comb line. Thus, the optical comb can be used as a reference for locking several tunable semiconductor lasers [58].

Pulsed technique

Mode locked laser diodes (MLLDs) have been regarded as promising candidates for signal sources in photonic radar systems, wireless data transmission, and frequency comb spectroscopy. They have the advantages of small size, low cost, high reliability, and low power consumption, thanks to semiconductor technology [18]. As shown in **Figure 6(a)**, MLLD structures have gain sections, biased with a direct current to achieve round trip unity gain in the steady state, and a number of reverse bias saturable absorber sections, which lock the optical modes in-phase so that the light is emitted in the form of optical pulses. Mode-locked optical pulses are generated from the complex dynamics between the gain and absorber sections that phase-lock the longitudinal modes of the cavity [19]. The gain section is usually a semiconductor optical amplifier (SOA), while the saturable absorber (SA) is an isolated short active section that is reverse biased. These sections are located within a laser cavity, defined by two mirrors, and the repetition rate of the optical pulse train is defined by the length of the laser cavity and the number of pulses circulating within the cavity. The Fourier transform of this pulse signal are RF tones at the fundamental frequency and its harmonics associated with the pulse repetition rate. Unwanted RF tones can easily be filtered out. One of the advantages of pulse signal generation is that it has been demonstrated to produce 7 dB higher radiated emitted power than heterodyning schemes [20]. The drawback is that since the repetition rate defined by a physical dimension of the device, the cavity length, the **frequency tuning range** is rather poor. Key parameters for optical signal generation application are the pulse duration, the achievable repetition rate and its tuning range as well as its stability.

The stability of a mode-locked laser, attributable to **coupled spontaneous emission and carrier density noise**, is conventionally quantified through timing jitter and amplitude noise. These magnitudes depend heavily on the mode-locked operating regime, which can either be passive or hybrid. Passive mode locking requires DC electrical bias to obtain the optical pulsed signal output, operating as an optical oscillator. The freedom from a need for RF input signals is a key advantage of the passive regime, however at the expense of signal stability [19]. The stability can be addressed by changing to a hybrid mode locking regime, in which the reverse-bias voltage is combined with a continuous wave (CW) signal at the fundamental frequency. It has been observed that the stability is inherited from the electronic source. The type of gain material used in the laser affects the phase noise, with quantum-dot being better than quantum well, and quantum-well being better than bulk material [21].

There are two widely used material platforms for producing integrated mode-locked lasers [22]. The most mature is the monolithic indium phosphide (InP) active-passive integration platform, which allows for combining various components such as semiconductor optical amplifiers, passive waveguides, on-chip mirrors, tunable distributed Bragg reflector gratings and phase shifters on the same chip with which to develop an integrated mode-locked structure [23]. The second is the more recently emerged heterogeneous silicon/III–V platform, which uses silicon-on-insulator (SOI) to provide passive devices and bonded III–V materials (typically grown on InP substrates) to provide the laser amplifier [24].

A crucial factor is how to define the laser cavity length, which defines the pulse train repetition rate. A common approach is to define the cavity through cleaved facet mirrors as shown in **Figure 6(b)**, which have two major drawbacks: (a) It prevents on-chip integration since the optical pulses exit from the facets of the chip, and (b) cleaving tolerance introduces cavity length uncertainty, which result in repetition rates variations from one device to another. Currently, different approaches have been demonstrated to integrate mode-locked laser diodes on-chip that benefit from the advantages of semiconductor manufacturing technology. One solution is to use ring resonators structures as shown in **Figure 6(c)** for InP and **Figure 6(d)** for silicon/III-V, offering lithographic control of the cavity length [25]. However, ring structures support two counterpropagating fields that bring complex interactions between them. Methods to suppress one of the propagation directions can either incorporate S-shaped structures [26] or introduce asymmetries [27] since the relative positioning of the amplifier and absorber in a monolithically integrated ring laser can be used to control the balance of power between counterpropagating fields in the mode-locked state. Another approach uses a cleaved facet on one end of the cavity and a distributed Bragg reflector (DBR) on the other end [28]. This technique has recently been improved, demonstrating mode-locking when a surface-etched grating is used [29], for a simpler fabrication process. Recently, a new approach to achieve on-chip laser sources has been demonstrated, defining the optical resonator by multimode interference reflectors (MIRs), which requires only a deep etch fabrication step [30]. Using this new approach, on-chip colliding pulse mode-locked laser

diode structures have been reported which avoids the cavity length uncertainty of monolithic structures that use cleaved facets. In addition, the saturable absorber, can be located at either ½ Lcav (at the center of the cavity) [31] or at ¼ Lcav (at one quarter of the total cavity length)[32], which increases the pulse repetition rate to two and four times the fundamental repetition rate respectively. Optical frequency combs with spacings reaching into the

millimeter-wave range (100 GHz) have been demonstrated through MLLD with 25 GHz fundamental repetition rate.

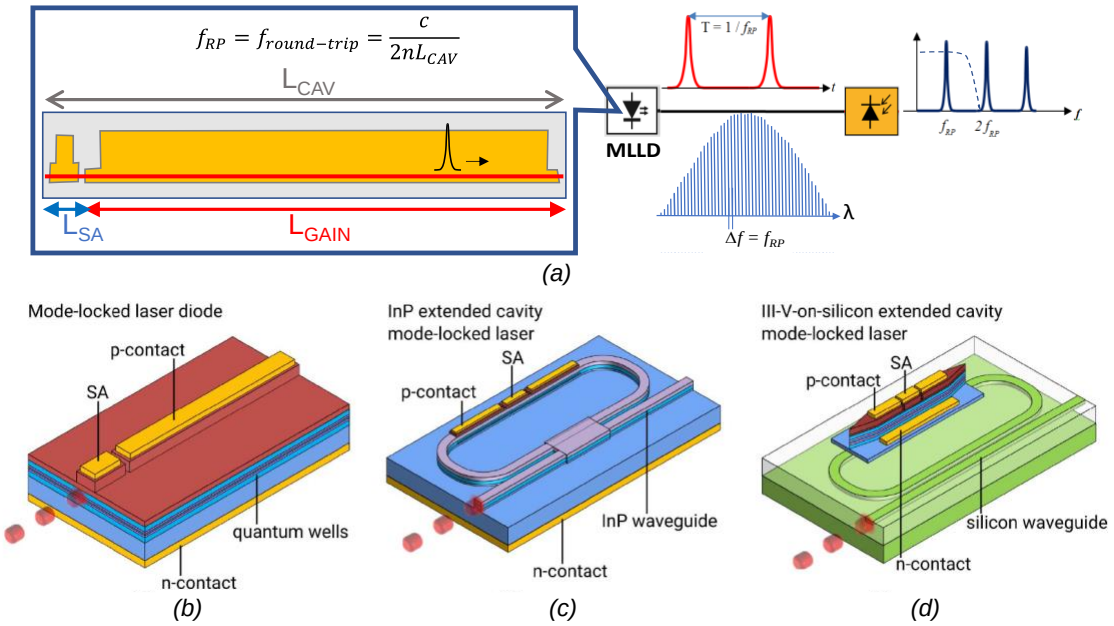

Figure 7 *(a) Key building blocks of photonic pulse signal generation system, including a mode-locked laser diode (MLLD) and a photodiode (PD), (b) monolithic InP quantum well laser diode [10], (c) monolithic InP active/passive photonic integrated extended cavity ring-type mode-locked laser diode and (d) III-V-on-silicon photonic integrated extended cavity ring-type mode-locked laser diode (partly from [22]).*

Figure 6 *Photonic integrated mode locked lasers: (a) with SA at center of cavity (½ Lcav), and (b) with SA at quarter length of cavity length (¼ Lcav).*

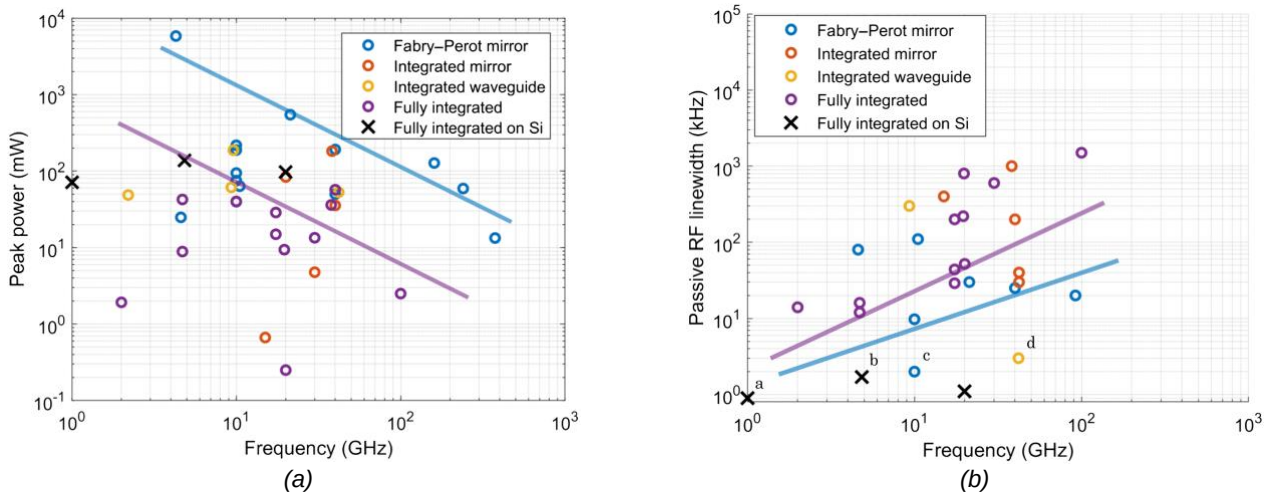

Figure 8 *Key parameters from mode-locked laser reported in literature using different integration approaches: (a) Peak power, and (b) RF linewidth. Fabry–Perot mirror: cleaved flat facets and single active amplifier waveguide, Integrated mirror: only an active waveguide with one or both mirrors on the chip, Integrated waveguide: has active and passive waveguides integrated on the chip, but flat facet mirrors, Fully integrated: structure includes both on-chip mirrors and integrated active and passive waveguides (from [24])*

For radar and radio communication applications, in addition to the generation of high-frequency RF tones with the help of photonic technologies, generation of actual radar pulses or analog radio communication signals at the desired RF carrier frequency can be achieved through the methods of photonic RF up- conversion and down-conversion [33]–[36]. An example consists of the use of a mode-locked laser (MLL). The laser output is modulated by a MZM driven by one or multiple IF signals placed at different IF frequencies. By suitably selecting the desired beating terms after photodetection, one can obtain up-conversion of each initial IF band to a desired carrier RF. Similarly, at the same transceiver, photonic down-conversion of a received RF signal can be achieved, as detailed in ***Figure 9***. This solution guarantees phase coherence among transmitted and received signals and among multiple RF-bands, which constitutes a key feature for coherent MIMO radar processing [37]. Indeed, coherent fusion of multiple radar detections from multiple radar sensors in a coherent centralized radar network architecture represents the most straightforward way to improve radar system performance in terms of cross-range resolution and the identification and classification capabilities. These features are now required, for example in the automotive field and in maritime traffic monitoring [37][38]. Such phase coherence among all signals involved in a radar network can be easily guaranteed by the use of photonics in both cases of employing a coherent optical spectral comb (e.g. a MLL) for photonic up- (and down)-conversion and when delivering radar signals in the RF domain, through Radio-over-Fiber (RoF) links to/from remote radar heads, as demonstrated in [37].

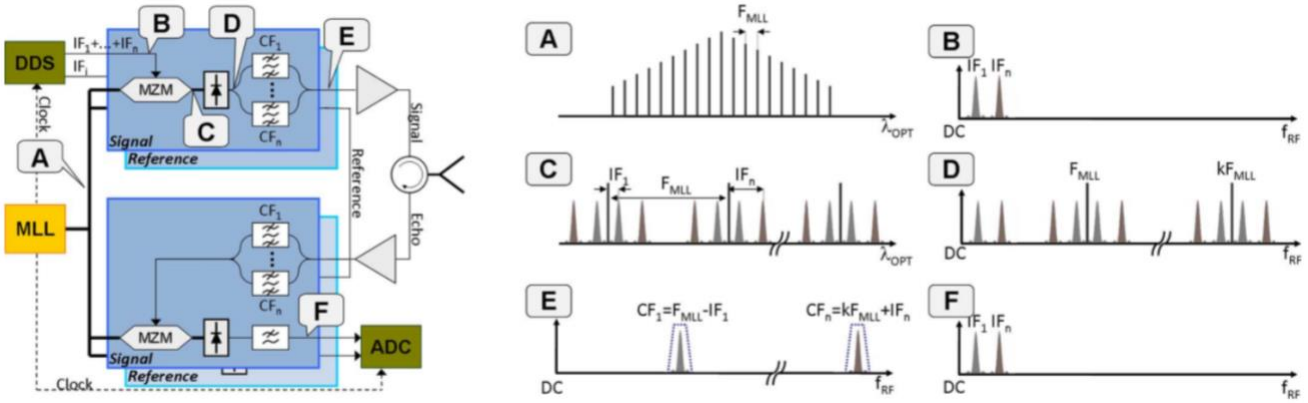

Figure 9*. (left) Scheme of principle of the multi-band photonic transceiver based on photonic up/down-conversion through the use of a MLL. (right) (A) Optical spectrum of the MLL. (B) Electrical spectrum of the modulating signal. (C) Optical spectrum after the MZM. (D) Electrical spectrum at the output of the PD. (E) Electrical spectrum after the filter bank. (F) Electrical spectrum of the echo signal at the receiver ADC.*

Opto-Electronic Oscillator

An alternative photonics-based method for generating RF signals uses an optoelectronic oscillator (OEO) to generate a tunable carrier frequency whose phase noise performance is not dependent on the value of that generated frequency. The generic schematic of an OEO is shown in ***Figure 10***. The employed optoelectronic modulator can be either a phase modulator or an intensity modulator depending on the particular implementation. The employed optical filter may act as a single or spectrally periodic bandpass filter, a spectral phase discontinuity or a notch filter, depending on the particular implementation. A tunable optical filter is used to achieve a tunable output frequency. The electrical loop may include specific amplifiers and/or filters, and the filter could be tunable. The electrical loop may include specific amplifiers and/or filters, and the filter could be tunable. The interesting aspects of all types of OEOs is that the phase noise performance of the obtained RF signal depends primarily on the phase noise of the employed CW laser source and the performance (mainly selectivity, Q-factor, thermal/mechanical stability, out-of-band rejection) of the employed optical filter. Given that the output RF carrier frequency is given by the spectral spacing between the CW laser mode and the optical filter center frequency (or free spectral range, in case of periodic filter), this means the phase noise performance can be independent of how high the generated carrier frequency. In addition, such a solution does not require a separate CW RF source to drive the modulator. Several implemented OEOs reveals excellent phase noise performance (in terms of dBc/Hz) for high offset frequencies, especially for

optical paths that have long, low-loss fiber or high-Q resonators for long storage times [39][40]. Compact integrated photonic OEOs have now been demonstrated [41]. For small frequency offsets (below 1–10 KHz), the phase noise power spectral density typically is determined by the phase noise of the electronic amplifier in the electrical loop. The phase noise at small frequency offsets can be reduced by using optical amplification in the optical loop instead of electronic amplification[42]. Furthermore, in this regime of low-frequency dynamics, PLL or post-processing techniques might be employed for mitigating the issue.

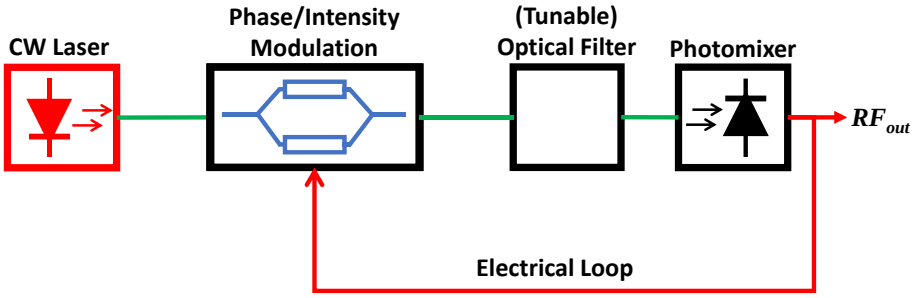

***Figure 10**. Schematic of an OEO.*

RF SIGNAL MODULATION TECHNOLOGIES

Optical modulators are the devices that encode the RF signal into the optical domain. As noted in [43], this is a key step in MWP systems, often determining the system performance, including bandwidth, system loss, linearity, and dynamic range. Thus, optical modulators play a very important role in MWP applications.

The simplest way to achieve optical modulation is by directly modulating the laser source. This generates an intensity modulated signal. While this scheme is attractive due to its simplicity (it only requires switching the laser on and off) the maximum modulation bandwidth is normally limited to 20-30 GHz since the modulation speed is limited by the relaxation oscillation of the laser. Although bandwidth as high as 55 GHz has been achieved with novel frequency-selective reflectors [44], this inherent limitation hinders the application of direct laser modulation to millimeter-wave and sub-THz photonic applications. Furthermore, due to the inherent coupling between the real and imaginary parts of the refractive index in semiconductors, direct modulation of lasers involves phase modulation of the signal. This results in the output signal being broadened in frequency (this effect is known as chirp) preventing its application in MWP applications where the optical signal must travel a long distance until it reaches the E/O converter (such as in radio-over-fiber) due to chromatic dispersion degradation.

The alternative method for modulation is using an external modulator. Since external modulators are electrically decoupled from the laser, their microwave design can be optimized independently from the laser in order to maximize speed. This allows external modulators to reach speeds much faster than that achieved with directly modulated lasers. The most popular external intensity modulators (IM) are the electro-absorption modulator (EAM) and the electro-optic Mach-Zehnder modulator (MZM). In the EAM, the applied voltage controls the absorption coefficient of the modulator's material, so that increasing voltages reduce the optical loss. On the other hand, in the MZM – which is formed by two parallel phase modulators forming an interferometer – the applied voltage varies the optical path difference between the two arms the interferometer. The MZM, thus, produces constructive interference when the phase of the light from these two paths are equal and destructive interference when those phases have a difference of one-half wavelength.

EAMs with bandwidths as high as 100 GHz have been demonstrated. However, due to their absorptive nature, EAMs present higher insertion losses than MZMs. This may render unacceptable link gain values and, thus, can affect the choice between MZM and EAM. Also, with EAMs, as with directly modulated lasers, the output signal is chirped, restricting their use to short-range MWP applications. MZMs, on the other hand, can be designed to have zero chirp, making them the preferred choice in medium and long-range MWP applications. Besides intensity

modulation, MWP applications also use phase modulators and complex modulators (also referred to as triple MZM), which are formed by two MZM in parallel nested inside a third modulator as shown in **Figure 11**. Complex modulators are used to generate single sideband signals (SSB) for example.

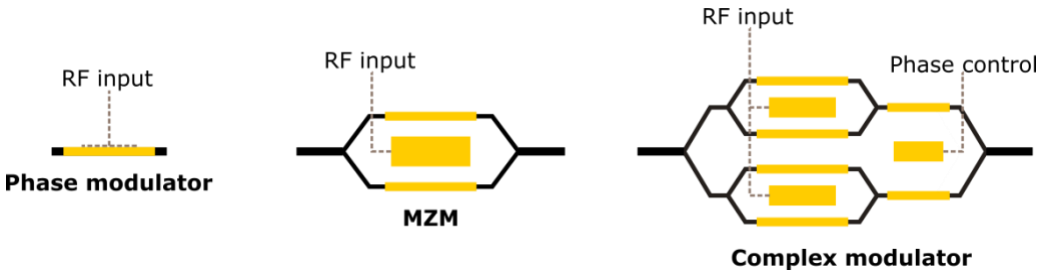

Figure 11. *Different types of modulators commonly used in MWP applications: the phase modulator, a MZM (consisting of two parallel modulators), and a complex modulator (consisting of two parallel MZM nested inside a third MZM).*

Table 1 *Selected modulators on different integration platforms*

Type	MZM					EAM	
Integration platform	NA (bulk LN)	Silicon-on-insulator	Thin-film LN (on silicon)	POH (on silicon)	InP	InP	GeSi
Bandwidth (GHz)	30	32	100	> 500	80	100	> 50
Driving voltage (V); DC extinction ratio (dB)	6; 22	7; 25	4.4; 30	3.4; 25	1.5; >25	2; >15	2; 4.2
Optical loss (dB)	3.5	6.8	< 0.5	13.6	2	3	4.4
Footprint (mm)	60	4.5	5	0.025	3.6	0.18	0.08
Reference	[45]	[46]	[47]	[48]	[49]	[50]	[51]

Table 1 shows a comparison of state-of-the-art MZM and EAMs in different integration platforms. As a reference we have also included a commercial modulator based on bulk (i.e., not suitable for integration) Lithium Niobate (LN). Both thin-film LN and plasmonic-organic hybrid (POH) MZMs have been proposed to push the modulation limits of integrated silicon modulators. Ultra-high speed data transmissions of up to 320 Gbit/s have been reported using thin-film LN modulators. On the other hand, POH modulators have demonstrated an unrivalled electro-optic bandwidth, with experiments showing no roll-off for frequencies up to 500 GHz. In POH modulators, however, a pending issue is optical losses, which remain high. Monolithic InP MZM modulators have also show very good performance, allowing modulation speeds of up to 80 GHz with low driving voltages. Monolithic EAMs with good performance have also been reported in InP and Si integrated photonics.

PHOTONIC RF SIGNAL PROCESSING TECHNOLOGIES

Photonic filtering

Microwave photonic filters are a photonic equivalent to RF filters, performing the same function in the optical domain as the microwave filter would do to an RF signal. The processing in the optical domain, however, brings the photonic-enabled advantages (i.e., low loss, high bandwidth, immunity to electromagnetic interference) and also enables reconfigurability of the filter functionality. Photonic filters have experienced a performance boost in the last two decades thanks to photonic integration, which is not only reducing the size, weight, and power consumption of optical filters but also improving their performance through an enhanced stability and the enabling of more-complex filter structures with reduced losses. While very high levels of functionality have been reported from photonic integrated filters in the recent years, it is vital that photonic techniques for RF filtering also match their electronic counterparts in the performance metrics highlighted in the introduction (i.e., link gain, noise figure and spurious-free dynamic range (SFDR)). The laser intensity noise, the modulator V_π and the optical filter insertion

loss greatly affect these metrics[43]. A recent review of integrated photonic filters and their comparison with respect to RF filters, in terms of these metrics and their functionality, was published in [52].

In terms of functionality, the development of material platforms with very low loss such as Silicon Nitride (Si_3N_4) (waveguide loss < 0.1 dB/cm) has paved the way towards the realization of ultra-high Q resonators. These resonators have been used to achieve filter cavities with MHz-level passbands widths [53]. Apart from Si_3N_4, other material platforms based on silicon substrates, such as silica and SOI, have been used to realize high-Q filters. A SOI distributed feedback resonator with a bandwidth of 2 GHz and a stopband of 1.2 THz was reported in [54]. In [55], a silica ring resonator with a Q factor exceeding 1 billion (10-GHz FSR and 220-kHz resonance width) was demonstrated.

Optical filters have also exploited the double sideband spectra generated after optical modulation. Depending on the type of modulator used before the filter (i.e., phase, MZM or complex modulator) and whether the processing is carried out in one or the two optical sidebands, different schemes have been reported (see ***Figure 12***). Using a Si_3N_4 ring resonator and two-symmetric-sideband processing, a resolution of 150 MHz and a link gain of 8 dB (highest link gain reported from an integrated photonic filter) was achieved [56]. Nonlinear effects have also been used in both Si_3N_4 and silica resonators to generate microcombs based on the Kerr effect. These combs have enabled the development of multi-wavelength transversal filters with a large number of taps. In [57], a Si_3N_4-based Kerr microcomb was used to build a transverse filter with 21 taps, achieving a passband with a full width half maximum (FWHM) of 1.1 GHz. In [58], 80 comb lines generated with a SOI ring were used to produce a filter with a filter passband bandwidth of 533 MHz. Recently, another nonlinear effect, stimulated Brillouin scattering (SBS), has been used in chalcogenide waveguides (which can be integrated with silicon) to achieve spectral resolutions down to 30 MHz [59].

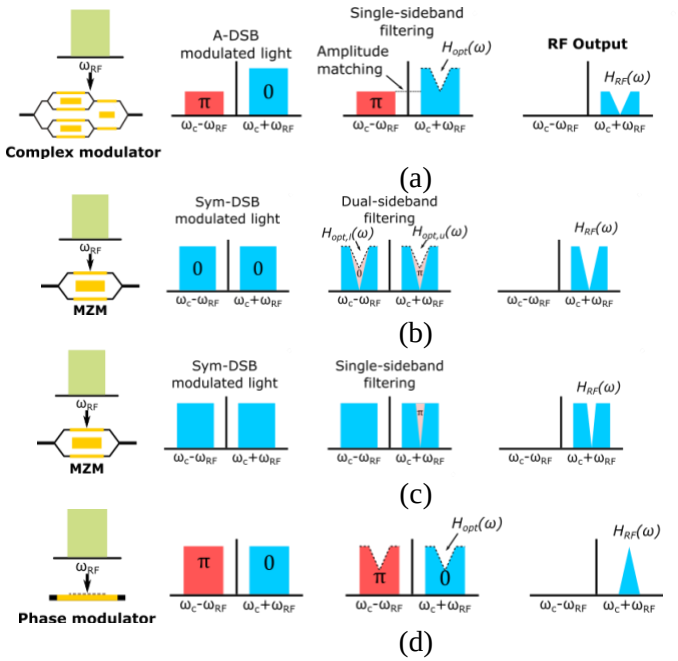

Figure 12 *Various types of MWP filters based on RF-Interference (Adapted from [2])*

While most of the photonic integrated circuits are currently designed for a specific application, a new approach is being developed to introduce integrated optical programmable processors [63]. The objective is to achieve a photonic equivalent to field programmable arrays (FPGAs). Such optical processors are built with a mesh of on-chip waveguides, tunable beam couplers and optical phase shifters that allows the processor to be programmed for a wide variety of functions (see ***Figure 13***).

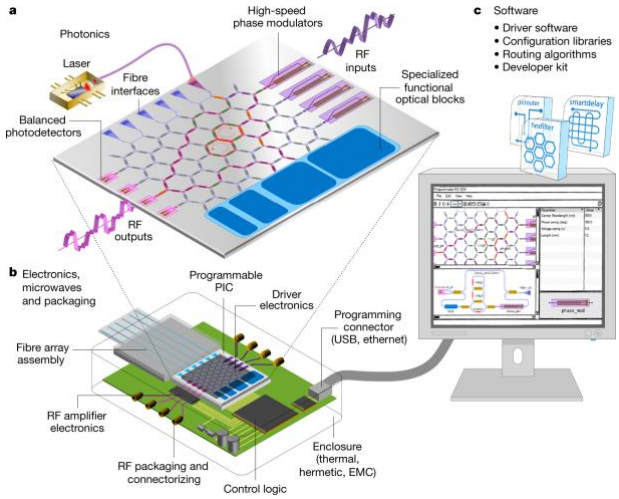

Figure 13 *Re-programmable photonic integrated circuit (From [63]).*

Optical beamforming networks

Optical beamforming networks (OBFNs) for steering and shaping RF electromagnetic waves through phased array antennas (PAAs) can be based either on optical phase shifters or true-time delay (TTD) elements. The use of phase shifters is simpler, but it is affected by the so-called squint effect, where different frequency components of the signal undergo different delays, distorting the beam shape or introducing a chromatic dispersion on the steering angle of the PAA radiation diagram. This issue eventually limits the maximum RF signal bandwidth. Phase shifters, however, offer easy tuneability, with dynamic response of tens of microseconds – in the case of thermal phase shifters – or up to the GHz-range, in case of fast doped pn-junctions. Integrated optical TTDs can be achieved through micro-ring resonators (MRRs). MRR-based TTDs allow a higher maximum RF signal bandwidth for a given amount of tolerable squint. The low loss of Si_3N_4 has allowed the fabrication of such TTDs networks that have a high number of channels and flat group delays over large bandwidths. This last feature is rather challenging to achieve in the RF domain, where beam formers are typically implemented using tunable phase shifters, which are intrinsically narrowband.

Photonic RF-spectrum monitoring

The precise detection and monitoring of the frequency spectrum of microwave signals are essential tasks for a broad range of applications, including telecommunications, radar, biomedical instrumentation, radio astronomy, etc. Current RF technologies suffer from a limited capability to provide agile (e.g., real-time) measurements over a large operation bandwidth in energy-efficient and compact (e.g., integrated) formats. These specifications are however increasingly desired in the above-mentioned application fields, particularly for platforms that require chip-scale integration and/or low weight and size, such as those involving satellites and drones. IMWP offers a promising path for realization of advanced real-time RF detection and analysis methods with broad tunability and high accuracy in integrated semiconductor technologies [64]. Towards this aim, solutions are being investigated that include (i) photonic implementation of broadband/multiband scanning RF receivers [65], [66]; (ii) devices for ultrarapid characterization of the full spectral content of RF signals, e.g., through optics-assisted frequency-to-time mapping [67], [68]; and (iii) photonic-based instantaneous frequency measurement systems [69], [70]. Work to date has demonstrated the unique potential of IMWP solutions to achieve the desired high performance, e.g., covering operation bandwidths in the tens-of-GHz range and above, with compact footprints. There are remaining important challenges to be addressed towards practical applications of these MWP solutions. These include the need to achieve significant improvements in some of the central specifications provided by these devices, such as concerning their frequency resolution and/or reliability, or the realization of crucial components not yet available in compact integrated formats, such as highly dispersive components for on-chip real-time RF spectral analysis. Research is also under steady progress to understand the potential of the MWP approach, and to optimize the resulting MWP system designs, to reach the needed performance in terms of important parameters, such as sensitivity and dynamic range under different noise conditions, and according to the specific requirements of the target applications.

Photonic Down-conversion

Apart from optical filtering, photonics can also be used for RF down-conversion. The device used for this is referred to as photo-mixer or photodetector. The typical configuration of a photonically-assisted RF receiver using this device is shown in ***Figure 14***. Photo-mixers are also used in O/E conversion, however, when they are used for RF down-conversion they have a twofold function: first, they provide the RF local oscillator (LO) (by mixing the two input optical signals) and second, perform the mixing of the RF LO with the incoming RF signal. By tuning the relative frequency of the two lasers driving the photo-mixer, this receiver can cover a wide range of carrier frequencies. The most common detector has been photoconductor devices [5], but photodiodes have also been used as a photonic down-converter [6][7]. Photoconductive devices are fabricated on Low Temperature GaAs (LT-GaAs), and more recently on InP and iron (Fe) doped InGaAs, not all of which are easily integrated. Novel types of photoconductors based on plasmonic effects [8], are currently being developed to enable RF Photonic transmitter and receiver integration on silicon.

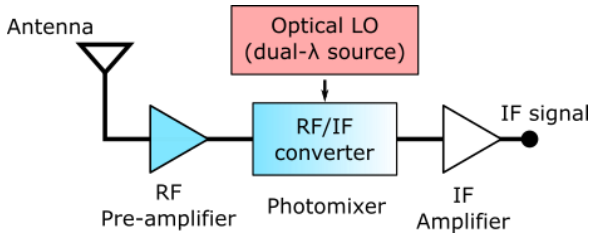

Figure 14 *Photonically-assisted RF recevier.*

PHOTOMIXER TECHNOLOGIES

O/E conversion is used in MWP transmitters to generate the RF signal and is used in MWP receivers to translate waveforms from the optical domain to the RF domain, typically as baseband or intermediate frequency (IF) waveforms, that can be processed further by electronic analog and digital circuits. Optoelectronic converters (also referred to as photodetectors) work as square law detectors where the generated photocurrent has a frequency equal to the difference between the input optical frequencies.

The most widely optoelectronic converter used in MWP applications is the p-i-n photodiode (PIN-PD), which is formed by an intrinsic absorption layer sandwiched between positively (p-type) and negatively (n-type) doped semiconductor layers. The most common PIN-PDs suitable for monolithic integration are based either in Ge-on-Si or in InP and lattice-matched III-V semiconductors (such as InGaAs). Both platforms can produce PIN-PD with good responsivity (~ 1 A/W), low dark currents (few nA), and relatively large bandwidth (> 30 GHz). State-of the-art, monolithically integrated Ge-on-Si and InP PIN-PDs can achieve bandwidths over 80 GHz [71][72]. For certain MWP applications, maximum RF power is also a key requirement. In PIN-PDs, however, there is a strong trade-off between RF power and bandwidth.

To exceed the limitations associated with PIN-PDs, the uni-travelling carrier photodiode (UTC-PD) was proposed. The main advantage of UTC-PDs compared to PIN-PDs is that only electrons contribute to the generated current. Since electrons have much higher drift velocities than holes, the transient time is reduced, allowing for a bandwidth increase. Furthermore, UTC-PDs offer reduced space-charge effects and, as a result, saturation occurs at higher levels of photocurrent relative to PIN-PDs. UTCs-PDs based on InP/InGaAs have led the way towards sub-THz MWP applications, showing unprecedented values of bandwidth and saturation power in photodiodes. A power above 100 μW was reported at a frequency of 264 GHz with a single discrete UTC-PD. Combining the output of two UTCs with a coplanar waveguide, a power up to 1 mW was obtained at a frequency of 300 GHz [73]. An alternative way of increasing the power from these devices is through spatial power combination with an array of antennas. This method has the advantage of not only summing the power of each element but also providing directional gain by concentrating the power in the transmission direction. Planar antennas integrated with UTC-PDs are attractive because large two-dimensional arrays with large number of antenna elements can be fabricated. As an example, in [74], a 4 × 1 UTC-PD-antenna array showing a directional gain of 6 dB at a frequency of 300 GHz was reported.

The epi-layer structure of an InP-based UTC-PD is very different from the structure of a laser or EA modulator. Thus, it is challenging to integrate the UTC-PD with other active components based on InP. However, the authors of [75] were able to fabricate a UTC-PD with techniques compatible with active-passive integration and which exhibited a -3-dB bandwidth of 170 GHz [75]. With this photodiode structure, a monolithically integrated tunable heterodyne source designed for the generation and modulation of mm-wave signals was demonstrated. The chip (shown in Fig. 4 (c)) included a pair of distributed feedback lasers, semiconductor optical amplifier amplifiers, passive waveguides, beam combiners, electro-optic modulators, and high-speed photodetectors on an InP-based platform. Millimeter wave generation at up to 105 GHz based on heterodyning the two optical wavelengths from the two integrated lasers has been achieved [12].

Recently, an intense research effort has been placed on another type of optoelectronic converter: the plasmonic photoconductor. Most of the demonstrations have focused on CMOS-compatible materials due to the prospects of achieving ultra-high speeds photodetection on this cost-effective technology platform. In **Error! Reference source not found.**, a silicon plasmonic photoconductor was reported with a bandwidth of 40 GHz and responsivity of 0.12 A/W. More recently, a plasmonic photoconductor based on Ge and with a frequency response of 100 GHz was published [77]. However, the dark current of the Ge-on-Si photodetectors has been higher than the dark current of the InGaAs/InP photodetectors.

Table 2 *Comparison of photodetectors*

Type	PIN-PD	PIN-PD	UTC-PD (with J-band waveguide output)	UTC-PD	Plasmonic photoconductor
Integration platform	Ge-on-Si	InGaAs/InP	NA	InGaAs/InP	Ge-on-Si
Bandwidth (GHz)	120	80	100 (around 264 GHz)	170	> 100
Responsivity (A/W)	0.8	0.55	0.27	0.27	0.38
Dark current (nA)	4×10^3 (-1 V)	5 (3 V)	-	-	$\sim18\times10^3$ (10 V)
Output power (dBm)	-	-	-8.7 (264 GHz)	-9 (200 GHz)	-
Reference	[71]	[72]	[73]	[75]	[77]

INTEGRATION ISSUES

Currently, the fabrication of photonic integrated circuits (PICs) is being shifted to a generic integration model. Within this model, photonic integration foundries fabricate PICs using Multi-Project Wafer (MPW) runs, where periodic productions are run over the year, with fixed tape-out dates in which several customers share the manufacturing costs of a whole wafer and thus reduce the prototype price. The fabrication process is fixed by the foundry, providing the platform Process Design Kit (PDK) which contains a library of devices for which the performance is known and optimized. Usually, every foundry specializes on one of the different photonic integration material substrates, being four main material platforms each one having its own advantages and disadvantages: Silica [78], Indium Phosphide (InP) [79], Silicon-On-Insulator (SOI) [80] and Silicon Nitride (Si_xN_y) [81].

It is a **challenge to optimize the diversity of active and passive components that are required for a given MWP system** using monolithic integration technology. A broad range of components may be required in a MWP system, including Distributed Feedback (DFB) lasers, Electro-Absorption Modulators (EAMs), Electro-optic Modulators (EOMs), Semiconductor Optical Amplifiers (SOA), Multimode Interference (MMI) couplers, waveguide time-delay paths, MicroRing-Resonators (MRR) and High-Speed Photodiodes (HS-PD). Thus, **it is of utmost importance to identify which photonic components should be integrated together**, based on the constraints of the intended application.

The reason for the variety of platforms is clear from the data shown in Table 3, from which is evident that there is no single platform that excels to host all the required functionalities. In fact, we observe that InP and SiN are

complementary, offering superior performance for active and for passive components, respectively. SOI enables compatibility with silicon electronics and more importantly, extremely fast plasmonic/organic modulators with 300-500 GHz bandwidth [83]. However, for the higher frequencies and also for the greater linearity needed for RF photonics, other materials may be more suitable than silicon. Thus, integration with silicon may not necessarily be that important for RF photonics that addresses millimeter-wave and sub-THz applications. Other substrates for high frequency is Polymer, a key material enabling optical micro-integration and which presents a low dielectric constant (2.4) compared to InP (12.4) and Si (11.9).

Table 3: *Performance comparison between four photonic integration platform technologies [82]*

Building Block	InP	SiP	SiN	Polymer
Passive components	●●	●●	●●●	●●
Polarisation components	●●	●●		●●●
Lasers	●●●	H	H	H
Phase modulators	●●●	P	●	●
Electro-Absorption modulators	●●●	●●		
Switches	●●●	●●	●	●●●
Optical Amplifiers	●●●	H	H	H
Detectors	●●●	H	H	H
Optical Isolators				H
RF and Microwave circuits	●	●	●	●●●
Substrate cost ($/cm2)	4.55	0.2		
Maximum size (mm)	150	450		

Performance	
●●●	Very good
●●	Good
●	Modest

Fabrication technology	
H	Hybrid
P	Plasmonic

Roadmap of Quantified Key Attribute Needs

Table X. Roadmap of Quantified Key Attribute Needs	[unit]	2020	2025	2030	2035	2040
Attribute 1						
Modulator E/O transduction efficiency						
Laser relative intensity noise						
Laser linewidth (and phase noise)						
Laser output power						
Laser power-conversion (wall-plug) efficiency						
Optical amplifier spontaneous emission noise						
Photodetector (or photomixer) responsivity						
Optical waveguide propagation loss						
Optical waveguide minimum bend radius						
Optical-fiber-interface coupling loss						
Temperature dependence of device performance						
Type of attributes B						
Attribute 2						

Critical (Infrastructure) Issues

Some important infrastructure issues include:

- Continued availability of III-V epitaxial materials,
- Wider availability of facilities that perform epitaxial regrowth.
- Wider availability of wafers that involve heterogeneous integration, such as III-V on silicon nitride on silicon, lithium niobate on insulator, or III-V on SOI.

- Facilities for semi-custom combined optical, RF and thermal packaging of integrated photonic chips into connectorized modules.

Technology Needs

PRIORITIZED RESEARCH NEEDS (AFTER 2025)

Table 1. Prioritized Research milestones (> 2025)	Relative priority
Source	
Uniform-intensity frequency combs with selectable lines and each line has Hz-level fundamental linewidth	Critical
Uniform-intensity frequency combs with high phase correlation between lines	Critical
High output power with high wall-plug efficiency	Critical
Investigation of quantum dot as gain medium for improved thermal stability, response and energy consumption	Desirable
Modulator	
Heterogeneous integration of silicon photonic materials (silicon, silicon nitride or silica) with materials that have a large EO coefficient, low optical loss and are compatible with high-temperature fabrication processes (such as III-V materials or lithium niobate).	Critical
Development of low-V_π, low-loss, >100 GHz modulators that are compatible with Si-photonic integration	Desirable
Optical signal processing unit	
Ultra-high resolution integrated and programmable filters with low loss (< 10 dB)	Critical
Generic RF photonic pulse shaper with tens-of-MHz tailorable resolutions	Critical
Generic-FPGA like RF photonic processor with low loss and low noise	Desirable
Deep Learning-RF photonic processor	Desirable
Broadly-tunable and highly-performing integrated RF photonic transceivers for spectral processing	Critical
O/E converter	
Increasing the output power up to 10 dBm at frequencies beyond 300 GHz.	Desirable
Optical routing	
Non-magnetic waveguide optical isolator / circulator integrated with the other photonic components	Critical

PRIORITIZED DEVELOPMENT & IMPLEMENTATION NEEDS (BEFORE OR DURING 2025)

Table 2. Prioritized Development & Implementation milestones (≤ 2025)	Relative priority
Source	
Ultra-narrow linewidth lasers with very-high central wavelength stability (maybe hybrid or Brillouin based)	Critical
Low-RIN (<-170 dB/Hz) and high-power lasers that can be integrated	Critical
High wall-plug efficiency (> 50%) and	Critical
High output power (> 1 Watt) supported by efficient heat-removal mechanisms	Desirable
Integrated optical isolator to maintain ultra-narrow linewidth lasers safe from back reflections	Critical
Modulator	
Low V_π (< 0.5 V) & high bandwidth (> 50 GHz) electro-optic modulators that can be large-scale integrated	Critical
Modulators with linearity comparable to the linearity of their electronic driver amplifiers	Critical
Optical Signal Processing Unit	
Development of high Q (exceeding 100 million) and ultra-low loss devices to increase spectral resolution of photonic filters	Critical
Low-loss (>0.05 dB/cm), long on-chip delay lines	Critical
Development of on-chip highly dispersive components	Critical
O/E converter	
Integration of ultrafast PD to PIC (heterogeneous integration of UTC-PD or PIN-PD & development of fast response GeSi PD)	Critical
Development of high-responsivity O/E converters with high saturation power	Critical
Waveguide coupled photodetector (O/E converter) that has both 100 GHz bandwidth and > 0.7 A/W responsivity.	Critical
Optical routing	
Ultra-low loss waveguiding circuits with small footprint	Critical
Compact waveguide switch with switching voltage of < 1 volt, prefer a latching switch that consumes zero stand-by power.	Critical
Waveguide optical isolator / circulator	Critical

Gaps and Showstoppers

The power consumption of the end-to-end microwave photonic solution must be comparable to or less than the power consumption of an electronic solution. Thus, parameters such as modulator Vpi and laser wall-plug efficiency are critical. Digital electronics may become MWP major contender in the future as analog-to-digital converters are getting better and the performance of electronic low-noise, wideband, high-linearity amplifiers is improving. Thus, the linearity and Vpi of the optical modulator is critical.

Since an integrated laser (and optical amplifier) generates so much heat, it is critical that this heat does not change the performance of the other photonic components, many of which depend on the effective refractive index of the waveguided optical modes and the resulting optical phase shifts. Having material with less temperature dependence or having effective ways to thermally isolate the heat generators from the temperature sensitive components is critical.

Electronic integrated circuits can be tested with on-wafer probes prior to being diced into chips. A microwave photonic circuit likewise could have on-wafer probe pads for the RF connections. But we also need on-wafer optical probing interfaces, such as low-loss grating couplers, to the optical waveguide circuit.

Recommendations on Potential Alternative Technologies

For a RF photonic system that is coupled to an antenna, an electronic low-noise amplifier could be used to connect the antenna to the optical modulators. In this case, it still is beneficial for the optical modulator to have sufficiently high modulation efficiency and low RF drive voltage so that a lower-power electronic amplifier can be used. This can result in lower overall power consumption for the system, especially the power consumption at the antenna unit. Similarly, an electronic high-power amplifier could be used to connect a photo-mixer to the antenna. The output power produced by the photo-mixer is preferably at a level for which the electronic amplifier can operate at its optimal power-added efficiency. In these cases, it is desirable to balance between the power and gain produced by the laser and/or by the optical amplifiers and the power and gain produced by the electronic amplifiers, so that the overall power consumption is minimized.

Contributors

Coordination:

Guillermo Carpintero, Professor, Universidad Carlos III de Madrid (ES)
Luis Gonzalez-Guerrero, Post-doctoral researcher, Universidad Carlos III de Madrid (ES)

Contributors:

Muhsin Ali – Universidad Carlos III de Madrid (ES)
Jose Azaña, Professor, Institut National de la Recherche Scientifique (INRS), Montreal, QC, Canada
Katarzyna Balakier – Airbus Defence and Space / University College London (UK)
Antonella Bogoni, Full Professor, Sant'Anna School of Advanced Studies and Director of Photonic Networks & Technologies National Laboratory, Interuniversity National Consortium for Telecommunications (CNIT)
Wolfgang Freude – Karlsruhe Institute of Technology (DE)
Gloria E. Höefler – Infinera Corporation (USA)
Antonio Malacarne, Photonic Networks & Technologies National Laboratory, Interuniversity National Consortium for Telecommunications (CNIT)
David Marpaung – University of Twente (NL)
Daniel Onori, Institut National de la Recherche Scientifique (INRS), Montreal, QC, Canada
Vitaly Rymanov – Microwave Photonics GmbH (DE)
Alwyn J. Seeds, Professor of Opto-electronics, Department of Electronic and Electrical Engineering, University College London
Andreas Stöhr – Professor at Universität Duisburg-Essen. Microwave Photonics GmbH (DE)
Paul W.L. Van Dijk – LioniX International (NL)
Daniel Yap, Senior Scientist, HRL Laboratories (US).

REFERENCES

[1] J. Capmany, D. Novak, "Microwave photonics combines two worlds," Nature Photon 1, 319–330 (2007). https://doi.org/10.1038/nphoton.2007.89

[2] D. Marpaung, J.Yao & J. Capmany, "Integrated microwave photonics". Nature Photon 13, 80–90 (2019). https://doi.org/10.1038/s41566-018-0310-5

[3] T. Nagatsuma and G. Carpintero, "Recent progress and future prospect of photonics-enabled terahertz communications research," IEICE Trans. Electron., vol. E98–C, pp.1060-1070, 2015.

[4] The European Network for High Performance Integrated Microwave Photonics (COST Action 16220) https://euimwp.eu/

[5] T. Harter, S. Ummethala, M. Blaicher, , *et al.*, "Wireless THz link with optoelectronic transmitter and receiver," Optica 6, 1063-1070 (2019)

[6] T. Nagatsuma, A. Kaino, S. Hisatake, K. Ajito, H.-J. Song, A. Wakatsuki, Y. Muramoto, N. Kukutsu, and Y. Kado, "Continuous-wave Terahertz Spectroscopy System Based on Photodiodes," PIERS Online, vol. 6, no. 4, pp. 390-394, 2010.

[7] E. Rouvalis, M. J. Fice, C.C. Renaud, A.J. Seeds, "Millimeter-wave optoelectronic mixers based on uni-traveling carrier Photodiodes," IEEE Trans. Microwave Theory and Techniques, Vol. 60, pp. 686-691, 2012.

[8] T. Harter, S. Muehlbrandt, S. Ummethala, *et al.* "Silicon–plasmonic integrated circuits for terahertz signal generation and coherent detection," *Nature Photon* **12,** 625–633 (2018).

[9] K. Balakier, L. Ponnampalam, M. J. Fice, C. C. Renaud and A. J. Seeds, "Integrated Semiconductor Laser Optical Phase Lock Loops," in IEEE Journal of Selected Topics in Quantum Electronics, vol. 24, no. 1, pp. 1-12, Jan.-Feb. 2018, Art no. 1500112, doi: 10.1109/JSTQE.2017.2711581.

[10] F. van Dijk, A. Accard, A. Enard, O. Drisse, D. Make and F. Lelarge, "Monolithic dual wavelength DFB lasers for narrow linewidth heterodyne beat-note generation," 2011 International Topical Meeting on Microwave Photonics, Singapore, pp. 73-76 (2011)

[11] R.T. Ramos, A.J. Seeds "Delay, linewidth and bandwidth limitations in optical phase-locked loop design" Electronics Letters Volume: 26 , Issue: 6: 1990 , Page(s): 389 – 39

[12] F. van Dijk et al., "Integrated InP heterodyne millimeterwave transmitter," IEEE Photon. Technol. Lett., vol. 26, no. 10, pp. 965–968, (2014).

[13] M. Sun et al., "Integrated four-wavelength DFB diode laser array for continuous-wave THZ generation," IEEE Photon. J., vol. 8, no. 4, pp. 1–8, (2016).

[14] J. Hulme et al., "Fully integrated microwave frequency synthesizer on heterogeneous silicon-iii/v," Opt. Express, vol. 25, no. 3, pp. 2422–2431, (2017).

[15] G. Carpintero, S. Hisatake, D. de Felipe, R.C. Guzman, T. Nagatsuma, N. Keil "Wireless Data Transmission at Terahertz Carrier Waves Generated from a Hybrid InP-Polymer Dual Tunable DBR Laser Photonic Integrated Circuit" Nature Scientific Reports Vol. 8, (2018)

[16] T. Komljenovic, D. Huang, P. Pintus, M. A. Tran, M. L. Davenport and J. E. Bowers, "Photonic Integrated Circuits Using Heterogeneous Integration on Silicon," in Proceedings of the IEEE, vol. 106, no. 12, pp. 2246-2257, Dec. 2018, doi: 10.1109/JPROC.2018.2864668.

[17] G. Qi, J. Yao, J. Seregelyi, S. Paquet and C. Bélisle, "Generation and Distribution of a Wide-Band Continuously Tunable Millimeter-Wave Signal With an Optical External Modulation Technique," IEEE Trans. Microw. Theory Tech., vol. 53, no. 10, pp. 3090-3097,(2005).

[18] T. Nagatsuma, N. Kukutsu, and Y. Kado, "Photonic Generation of Millimeter and Terahertz Waves and Its Applications," Applied Electromagnetics and Communications ICECom, Dubrovnik, 2007, pp. 1-4.

[19] K.A. Williams, M.G. Thompson, and I.H. White, "Long-wavelength monolithic mode-locked diode lasers," New J. Phys. 6, 179 (2004).

[20] L. Moeller, A. Shen, C. Caillaud, and M. Achouche, “Enhanced THz generation for wireless communications using short optical pulses, ” In Infrared, Millimeter, and Terahertz Waves (IRMMW-THz), 2013, pp. 1-3.

[21] G. Carpintero, M. G. Thompson, R. V. Penty, and I. H. White, “Low noise performance of passively mode-locked 10-GHz quantum-dot laser diode,” IEEE Photon. Technol. Lett., vol. 21, no. 6, pp. 389–391, March 2009.

[22] K. Van Gasse et al., "Recent Advances in the Photonic Integration of Mode-Locked Laser Diodes," in IEEE Photonics Technology Letters, vol. 31, no. 23, pp. 1870-1873, (1 Dec.1, 2019)

[23] V. Moskalenko, K. Williams, and E. Bente, "Mode-locked lasers in InP active-passive integration platforms," in *Asia Communications and Photonics Conference (ACPC) 2019*, OSA Technical Digest (Optical Society of America, 2019), paper M3E.5.

[24] Michael L. Davenport, Songtao Liu, and John E. Bowers, "Integrated heterogeneous silicon/III–V mode-locked lasers," Photon. Res. 6, 468-478 (2018)

[25] J. P. Hohimer and G. A. Vawter, “Passive mode locking of monolithic semiconductor ring lasers at 86 GHz,” Appl. Phys. Lett. 63, pp. 1598–1600 (1993).

[26] H. Cao, H. Deng, H. Ling, C. Liu, V. A. Smagley, R. B. Caldwell, G. Smolyakov, A. L. Gray, L. F. Lester, P. G. Eliseev, and M. Osinski, “Unidirectional operation of quantum-dot ring lasers,” in Conference on Lasers and Electro-Optics (CLEO) (2005), Vol. 3, pp. 1793–1795.

[27] M. Tahvili, Y. Barbarin, X. Leijtens, T. de Vries, E. Smalbrugge, J. Bolk, H. Ambrosius, M. Smit, and E. Bente, “Directional control of optical power in integrated InP/InGaAsP extended cavity mode-locked ring lasers,” Opt. Lett. 36, 2462–2464 (2011).

[28] S. Joshi, N. Chimot, R. Rosales, S. Barbet, A. Accard, A. Ramdane, and F. Lelarge, “Mode locked InAs/InP quantum dash based DBR Laser monolithically integrated with a semiconductor optical amplifier,” in International Conference on Indium Phosphide and Related Materials (IPRM) (2013).

[29] L. Hou, M. Haji, and J. H. Marsh, “Monolithic mode-locked laser with an integrated optical amplifier for low-noise and high power operation,” IEEE J. Sel. Top. Quantum Electron. 19, 1100808 (2013).

[30] E. Kleijn, M. K. Smit, and X. J. M. Leijtens, “Multimode interference reflectors: a new class of components for photonic integrated circuits,” J. Lightwave Technol. 31, 3055–3063 (2013).

[31] C. Gordón, R. Guzmán, X. Leijtens, and G. Carpintero, "On-chip mode-locked laser diode structure using multimode interference reflectors," Photon. Res. 3, 15-18 (2015)

[32] C. Gordón, R. Guzmán, V. Corral, M. Chieh Lo and G. Carpintero, "On-Chip Multiple Colliding Pulse Mode-Locked Semiconductor Laser," in Journal of Lightwave Technology, vol. 34, no. 20, pp. 4722-4728, 15 Oct.15, 2016, doi: 10.1109/JLT.2016.2553640.

[33] Ghelfi, P., Laghezza, F., Scotti, F. et al. A fully photonics-based coherent radar system. Nature 507, 341–345 (2014).

[34] F. Scotti, F. Laghezza, P. Ghelfi and A. Bogoni, "Multi-Band Software-Defined Coherent Radar Based on a Single Photonic Transceiver," in IEEE Transactions on Microwave Theory and Techniques, vol. 63, no. 2, pp. 546-552, Feb. 2015.

[35] P. Ghelfi, F. Laghezza, F. Scotti, D. Onori and A. Bogoni, "Photonics for Radars Operating on Multiple Coherent Bands," in Journal of Lightwave Technology, vol. 34, no. 2, pp. 500-507, 15 Jan.15, 2016.

[36] G. Serafino, S. Maresca, C. Porzi, F. Scotti, P. Ghelfi and A. Bogoni, "Microwave Photonics for Remote Sensing: From Basic Concepts to High-Level Functionalities," in Journal of Lightwave Technology, vol. 38, no. 19, pp. 5339-5355, 1 Oct.1, 2020.

[37] A. Malacarne, S. Maresca, F. Scotti, P. Ghelfi, G. Serafino and A. Bogoni, "Coherent Dual-Band Radar-Over-Fiber Network With VCSEL-Based Signal Distribution," in Journal of Lightwave Technology, vol. 38, no. 22, pp. 6257-6264, 15 Nov.15, 2020.

[38] F. Scotti, S. Maresca, L. Lembo, G. Serafino, A. Bogoni and P. Ghelfi, "Widely Distributed Photonics-Based Dual-Band MIMO Radar for Harbour Surveillance," in IEEE Photonics Technology Letters, vol. 32, no. 17, pp. 1081-1084, 1 Sept.1, 2020.

[39] L. Maleki, "The opto-electronic oscillator (OEO): Review and recent progress," 2012 European Frequency and Time Forum, p. 497-500, IEEE.

[40] O. Lelievre, et al., "A model for designing ultralow noise single- and dual-loop 10-GHz optoelectronic oscillators," J. Lightwave Tecnology, v. 35, n. 20, October 15, 2017, p. 4366-4374.

[41] P. T. Do, et al., "Wideband tunable microwave signal generation in a silicon-microring-based optoelectronic oscillator," Nature Scientific Reports, v. 10 (2020).

[42] P. S. Devgan, V. J. Urick, J. F. Diehl and K. J. Williams, "Improvement in the phase noise of a 10 GHz optoelectronic oscillator using all-photonic gain," J. Lightwave Technology, v. 27, n. 15, August 1, 2009, pp. 3189-3193.

[43] V. J. Urick, et al., "Wideband analog photonic links: Some performance limits and considerations for multi-octave implementation," Proceedings of SPIE, Volume 8259, p. 825904 (2012).

[44] Y. Matsui, et al., "55 GHz bandwidth distributed reflector laser," J. Lightwave Technology, v. 35, n. 3, February 1, 2017, p. 397-403.

[45] IXblue: https://photonics.ixblue.com/store/lithium-niobate-electro-optic-modulator/intensity-modulators#:~:text=iXblue%20offers%20the%20most%20comprehensive,1550%20nm%20and%202%20microns.

[46] J. Lin, H. Sepehrian, L. A. Rusch, and W. Shi, "Single-carrier 72 GBaud 32QAM and 84 GBaud 16QAM transmission using a SiP IQ modulator with joint digital-optical pre-compensation," *Optics Express*, vol. 27, no. 4, p. 5610, Feb. 2019, doi: 10.1364/oe.27.005610.

[47] C. Wang *et al.*, "Integrated lithium niobate electro-optic modulators operating at CMOS-compatible voltages," *Nature*, vol. 562, no. 7725, pp. 101–104, Oct. 2018, doi: 10.1038/s41586-018-0551-y.

[48] W. Heni *et al.*, "108 Gbit/s Plasmonic Mach-Zehnder Modulator with > 70-GHz Electrical Bandwidth," *Journal of Lightwave Technology*, vol. 34, no. 2, pp. 393–400, Jan. 2016, doi: 10.1109/JLT.2015.2487560.

[49] Y. Ogiso *et al.*, "Ultra-High Bandwidth InP IQ Modulator for Beyond 100-GBd transmission," 2019.

[50] M. Chaciński, U. Westergren, R. Schatz, B. Stoltz, S. Hammerfeldt, and L. Thylén, "Monolithically integrated 100 GHz DFB-TWEAM," Journal of Lightwave Technology, vol. 27, no. 16, pp. 3410–3415, Aug. 2009, doi: 10.1109/JLT.2009.2015773.

[51] S. A. Srinivasan et al., "50Gb/s C-band GeSi Waveguide Electro-Absorption Modulator."

[52] Y. Liu, A. Choudhary, D. Marpaung, and B. J. Eggleton, "Integrated microwave photonic filters," Advances in Optics and Photonics, vol. 12, no. 2, p. 485, Jun. 2020, doi: 10.1364/aop.378686.

[53] C. Taddei, L. Zhuang, C. G. H. Roeloffzen, M. Hoekman, and K. J. Boller, "High-Selectivity On-Chip Optical Bandpass Filter with Sub-100-MHz Flat-Top and Under-2 Shape Factor," IEEE Photonics Technology Letters, vol. 31, no. 6, pp. 455–458, Mar. 2019, doi: 10.1109/LPT.2019.2897859.

[54] C. Porzi, G. J. Sharp, M. Sorel, and A. Bogoni, "Silicon Photonics High-Order Distributed Feedback Resonators Filters," IEEE Journal of Quantum Electronics, vol. 56, no. 1, Feb. 2020, doi: 10.1109/JQE.2019.2960560.

[55] L. Wu et al., "Greater than one billion Q factor for on-chip microresonators," Optics Letters, vol. 45, no. 18, p. 5129, Sep. 2020, doi: 10.1364/ol.394940.

[56] Y. Liu, J. Hotten, A. Choudhary, B. J. Eggleton, and D. Marpaung, "All-optimized integrated RF photonic notch filter," Optics Letters, vol. 42, no. 22, p. 4631, Nov. 2017, doi: 10.1364/ol.42.004631.

[57] X. Xue *et al.*, "Programmable single-bandpass photonic rf filter based on kerr comb from a microring," *Journal of Lightwave Technology*, vol. 32, no. 20, pp. 3557–3565, Oct. 2014, doi: 10.1109/JLT.2014.2312359.

[58] X. Xu *et al.*, "Advanced Adaptive Photonic RF Filters with 80 Taps Based on an Integrated Optical Micro-Comb Source," *Journal of Lightwave Technology*, vol. 37, no. 4, pp. 1288–1295, Feb. 2019, doi: 10.1109/JLT.2019.2892158.

[59] D. Marpaung *et al.*, "Low-power, chip-based stimulated Brillouin scattering microwave photonic filter with ultrahigh selectivity," *Optica*, vol. 2, no. 2, p. 76, Feb. 2015, doi: 10.1364/optica.2.000076.

[60] D. Marpaung *et al.*, "Si_3N_4 ring resonator-based microwave photonic notch filter with an ultrahigh peak rejection," *Optics Express*, vol. 21, no. 20, p. 23286, Oct. 2013, doi: 10.1364/oe.21.023286.

[61] Y. Liu, D. Marpaung, A. Choudhary, and B. J. Eggleton, "Lossless and high-resolution RF photonic notch filter," *Optics Letters*, vol. 41, no. 22, p. 5306, Nov. 2016, doi: 10.1364/ol.41.005306.

[62] J. Palací, G. E. Villanueva, J. V. Galán, J. Martí, and B. Vidal, "Single bandpass photonic microwave filter based on a notch ring resonator," *IEEE Photonics Technology Letters*, vol. 22, no. 17, pp. 1276–1278, 2010, doi: 10.1109/LPT.2010.2053527.

[63] Bogaerts, W., Pérez, D., Capmany, J. et al. Programmable photonic circuits. Nature 586, 207–216 (2020). https://doi.org/10.1038/s41586-020-2764-0

[64] Luis Romero Cortés, Daniel Onori, Hugues Guillet de Chatellus, Maurizio Burla, and José Azaña, "Towards on-chip photonic-assisted radio-frequency spectral measurement and monitoring," Optica 7, 434-447 (2020).

[65] D. Onori et al., "A Photonically-enabled Compact 0.5-26.5 GHz RF Scanning Receiver," Journal of Lightwave Technology, vol. 36, pp. 1831-1839, 2018.

[66] D. Onori, A. Samani, D. V. Plant, and J. Azaña, "An RF scanning receiver on a silicon photonic chip," in IEEE International Topical Meeting on Microwave Photonics (2019).

[67] C. Wang and J. Yao, "Ultrahigh-resolution photonic-assisted microwave frequency identification based on temporal channelization," IEEE Trans. Microw. Theory Tech. 61, 4275–4282 (2013).

[68] S. Reddy Konatham, R. Maram, L. Romero Cortés, J. H. Chang, L. Rusch, S. LaRochelle, H. Guillet de Chatellus, J. Azaña, "Real-time gap-free dynamic waveform spectral analysis with nanosecond resolutions through analog signal processing," *Nature Commun.*, vol. 11, article #3309 (pp. 1-12) (2020).

[69] D. Marpaung, "On-chip photonic-assisted instantaneous microwave frequency measurement system," IEEE Photon. Technol. Lett. 25, 837–840 (2013).

[70] M. Burla, X. Wang, M. Li, L. Chrostowski, and J. Azaña, "Wideband dynamic microwave frequency identification system using a low-power ultracompact silicon photonic chip," Nat. Commun. 7, 13004 (2016).

[71] Laurent Vivien et al., "Zero-bias 40Gbit/s germanium waveguide photodetector on silicon," Optics Express, vol. 19, no. 11, p. 1096, 2011.

[72] P. Runge et al., "80GHz balanced photodetector chip for next generation optical networks," 2014, doi: 10.1364/ofc.2014.m2g.3.

[73] H. Ito, T. Furuta, Y. Muramoto, T. Ito, and T. Ishibashi, "Photonic millimetre- and sub-millimetre-wave generation using J-band rectangular-waveguide-output uni-travelling-carrier photodiode module," Electronics Letters, vol. 42, no. 24, pp. 1424–1425, 2006, doi: 10.1049/el:20063033.

[74] G. Sakano, J. Haruki, K. Sakuma and K. Kato, "4-channel synchronous THz-wave generatorcomposed of arrayed UTC-PDs and antennas," 2016 21st OptoElectronics and Communications Conference (OECC) held jointly with 2016 International Conference on Photonics in Switching (PS), Niigata, Japan, 2016, pp. 1-3.

[75] E. Rouvalis *et al.*, "170 GHz uni-traveling carrier photodiodes for InP-based photonic integrated circuits," *OPTICS EXPRESS 20090*, vol. 58, no. 11, pp. 1716–1718, 2010.

[76] Harter, T.; Füllner, C.; Kemal, J. N.; Ummethala, S.; Steinmann, J. L.; Brosi, M.; Hesler, J. L.; Bründermann, E.; Müller, A.-S.; Freude, W.; Randel, S.; Koos, C.: 'Generalized Kramers–Kronig receiver for coherent terahertz communications,' Nature Photon. 14 (2020) 601–606

[77] Y. Salamin et al., "100 GHz Plasmonic Photodetector," ACS Photonics, vol. 5, no. 8, pp. 3291–3297, Aug. 2018, doi: 10.1021/acsphotonics.8b00525.

[78] G. C. Righini and A. Chiappini, "Glass optical waveguides: a review of fabrication techniques," Optical Engineering, vol. 53, no. 7, p. 071 819, (2014).

[79] M. Smit, K. Williams, and J. Van Der Tol, "Past, present, and future of InP-based photonic integration," APL Photonics, vol. 4, no. 5, p. 050 901, (2019).

[80] R. Soref, "The past, present, and future of silicon photonics," IEEE Journal of Selected Topics in Quantum Electronics, vol. 12, no. 6, pp. 1678–1687, (2006).

[81] Roeloffzen, C. G. H., Zhuang, L., Taddei, C., Leinse, A., Heideman, R. G., van Dijk, P. W. L., Oldenbeuving, R. M., Marpaung, D. A. I., Burla, M., & Boller, K-J. "Silicon nitride microwave photonic circuits" *Optics express, 21*(19), 22937-22961 (2013)

[82] Following Table 5 (pag. 27) of "JePPIX Roadmap 2018: The road to a multi-billion euro market in Integrated Photonics", including polymer substrate of Hybrid Integration Group at FhG-HHI.

[83] M. Burla, et al., "500 GHz plasmonic Mach-Zehnder modulator enabling sub-THz microwave photonics," APL Photonics, v. 4, p. 056106 (2019).